Electron-phonon coupling and superconductivity in the (4/3)-monolayer of Pb on Si(111): Role of spin-orbit interaction

I. Yu. Sklyadneva,[1,2,3,4] R. Heid,[2] K.-P. Bohnen,[2] P. M. Echenique,[1,5,6] and E. V. Chulkov[5,6,7]

[1]*Donostia International Physics Center (DIPC), 20018 San Sebastián/Donostia, Basque Country, Spain*

[2]*Institut für Festkörperphysik, Karlsruher Institut für Technologie, D-76021 Karlsruhe, Germany*

[3]*Institute of Strength Physics and Materials Science, pr. Academicheskii 2/1,634021, Tomsk, Russian Federation*

[4]*Tomsk State University, 634050, Tomsk, Russian Federation*

[5]*Departamento de Física de Materiales, Facultad de Ciencias Químicas, UPV/EHU,*

Apdo. 1072, 20080 San Sebastián/Donostia, Basque Country, Spain

[6]*Centro de Física de Materiales CFM - Materials Physics Center MPC, Centro Mixto CSIC-UPV/EHU, 20018 San Sebastian/Donostia, Spain*

[7]*St. Petersburg State University, 199034, St. Petersburg, Russian Federation*

The effect of spin-orbit coupling on the electron-phonon interaction in a (4/3)-monolayer of Pb on Si(111) is investigated within the density-functional theory and linear-response approach in the mixed-basis pseudopotential representation. We show that the spin-orbit interaction produces a large weakening of the electron-phonon coupling strength, which appears to be strongly overestimated in the scalar relativistic calculations. The effect of spin-orbit interaction is largely determined by the induced modification of Pb electronic bands and a stiffening of the low-energy part of phonon spectrum, which favor a weakening of the electron-phonon coupling strength. The state-dependent strength of the electron-phonon interaction in occupied Pb electronic bands varies depending on binding energy rather than electronic momentum. It is markedly larger than the value averaged over electron momentum because substrate electronic bands make a small contribution to the phonon-mediated scattering and agrees well with the experimental data.

I. INTRODUCTION

Ultrathin metallic films grown on semiconductor substrates have attracted much attention due to their two-dimensional (2D) physical properties [1–4]. Lead deposited on a silicon substrate forms a well-defined interface due to the low mutual solubility of Pb and Si [5] thereby representing a model system for investigating metal-semiconductor interfacial properties. The superconductivity of Pb films grown on Si(111) [6–9] has stimulated an active interest in thin Pb films too [10–15]. Scanning tunneling microscopy measurements (STM) demonstrated that superconductivity exists even at 2D limit in a single layer of Pb on Si(111) [3].

The experimental findings inspired a great amount of theoretical work focused on thin Pb film properties such as the critical temperature of superconductivity [9,16,17] or the strength of the electron-phonon (e-ph) interaction [18–22]. The e-ph coupling parameter in thin Pb films on silicon was estimated both experimentally and theoretically for the highest occupied quantum-well states [23,24]. As for the strength of e-ph interaction averaged over electron momentum, it was mainly studied at the Fermi level (E_F) of freestanding Pb(111) films using both scalar relativistic [9,19,21] and including spin-orbit coupling (SOC) calculations [22]. However, in the experiments Pb films are grown on a silicon substrate and the substrate is expected to be very important for small adlayer thicknesses and evidently influence superconductivity in ultrathin Pb films [12,16,17,24].

Ab initio calculations for Si-substrate-supported lead films were carried out for the (1×1) Pb/Si(111) films of various thicknesses [21] as well as for a (4/3)-monolayer of Pb on Si(111) [20,21]. Both calculations were performed without taking into account the spin-orbit interaction. The superconduction transition temperature, T_c, estimated in the scalar relativistic calculations turned out to be in agreement with the experimental value for a (4/3)-monolayer of Pb [3]. So it was believed that SOC does not affect the final results.

However, it is known that the spin-orbit interaction has a profound impact on the e-ph coupling both in bulk Pb [25,26] and in freestanding Pb films of various thicknesses [22]. We intend to show that SOC is very important for an accurate quantitative description of the e-ph interaction in Si-supported Pb films too and the perfect coincidence between the theoretical and experimental values of T_c looks accidental because of the overestimation of the e-ph coupling strength in the scalar relativistic calculations [20,21]. Another question is whether the positions of E_F in the experiment [3] and in the calculations coincide with respect to the substrate valence band edge because the critical temperature, T_c is measured (and calculated) at the Fermi level.

Here we present a first-principles study of the effect of spin-orbit interaction on the pairing strength in the phonon-induced scattering processes. We focus on the (4/3)-monolayer (ML) of Pb on Si(111) forming a dense phase with the $\sqrt{3} \times \sqrt{3}$ unit cell, which was found to be superconducting with transition temperature of 1.83 K [3]. The calculations of the

electron-phonon coupling strength averaged over electron momentum, $\lambda(E)$, were carried out at the Fermi energy as well as at energies below and above E_F to estimate the effect of variations in the electronic density of states, $N(E)$, on $\lambda(E)$. We also analyze the state-dependent strength of electron-phonon interaction in occupied Pb electronic bands.

II. CALCULATION DETAILS

A. Method

The strength of electron-phonon interaction averaged over electron momentum at fixed energy E is defined as [29]

$$\lambda(E) = 2 \int_0^\infty \frac{\alpha^2 F(E; \omega)}{\omega} \, d\omega. \tag{1}$$

Here $\alpha^2 F(E; \omega)$ is the Eliashberg spectral function:

$$\alpha^2 F(E; \omega) = \frac{1}{\hbar N(E)} \sum_{\mathbf{q}, \nu} \delta(\omega - \omega_{\mathbf{q}\nu}) \sum_{\mathbf{k}, i, f} \delta(\epsilon_{\mathbf{k}i} - E)$$

$$\times \left| g_{\mathbf{k}+\mathbf{q}f, \mathbf{k}i}^{\mathbf{q}\nu} \right|^2 \delta(\epsilon_{\mathbf{k}+\mathbf{q}f} - E), \tag{2}$$

where $g_{\mathbf{k}+\mathbf{q}f, \mathbf{k}i}^{\mathbf{q}\nu}$ is the e-ph matrix element, $\epsilon_{\mathbf{k}i}$ and $\epsilon_{\mathbf{k}+\mathbf{q}f}$ are energies of initial (i) and final (f) electronic states, and $N(E)$ is the density of electronic states. The summation is carried out over (i) all combinations of electronic states ($\mathbf{k}i$) and ($\mathbf{k} + \mathbf{q}f$) and (ii) phonon modes ($\mathbf{q}, \nu$). To average the e-ph parameter over electron momentum, a dense ($48 \times 48 \times 1$) **k**-point mesh corresponding to 217 special points in the irreducible part of the surface Brillouin zone (SBZ) was used. In the self-consistent calculations the Brillouin zone integrations were performed by sampling a uniform ($12 \times 12 \times 1$) **k**-point mesh and a Gaussian smearing scheme with a width of 0.05 eV.

All calculation were carried out within the density-functional formalism and the local density approximation (LDA) [30] using norm-conserving pseudopotentials (PP) [31] and the mixed-basis approach [32,33]. Details of the spin-orbit coupling implementation within the mixed-basis PP method can be found in Ref. [25]. Dynamical properties were calculated using the linear response technique [34,35].

B. Structural parameters

The silicon substrate is modeled by periodically repeating films consisting of six Si(111) layers (a three-bilayer film) and separated by a vacuum gap of ~12 Å. In principle, a substrate consisting of two Si bilayers is already sufficient to reproduce the structural parameters and the band dispersion in good agreement with the data obtained for a six-bilayer Si film [27]. For three Si bilayer, used in our calculations, the bond lengths are completely converged with an accuracy of less than 0.01 Å. Lead atoms are then deposited on the top of the substrate, and the bottom of the film is passivated by hydrogen atoms to saturate the silicon dangling bonds. The lattice constant is first fixed at the theoretical bulk Si lattice parameter $a = 5.402$ Å obtained by total-energy minimization, which is a bit smaller compared to the experimental value [36], $a_{\text{exp}} = 5.43$ Å. A superstructure formed by (4/3)-ML of Pb on Si(111), a dense ($\sqrt{3} \times \sqrt{3}$) phase (the so called H₃ structure) has four Pb atoms
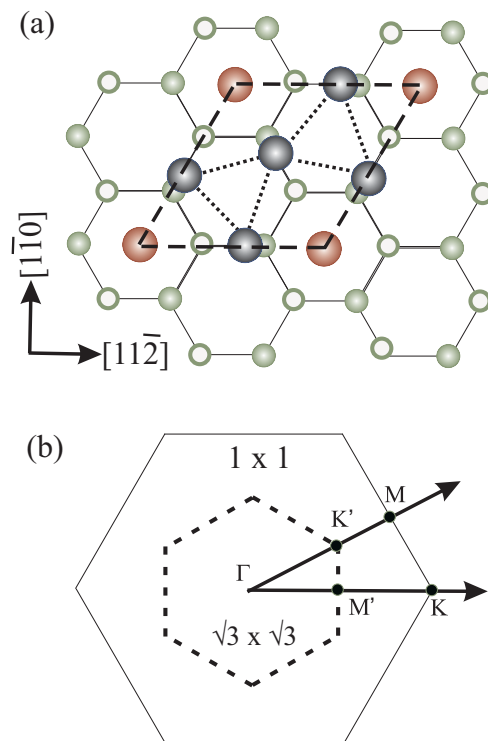

FIG. 1. (a) Top view of the (4/3)-ML of Pb on Si(111) (H₃). Big circles correspond to Pb atoms. Si atoms are shown by full (in the first substrate layer, Si₁) and open (in the second layer, Si₂) small circles. The color assignments are as follows: brown, Pb atom in the hollow H₃ site; black, Pb atoms forming a trimer at off-centered T_1 sites; green, Si atoms of the substrate. The dashed line indicates the $\sqrt{3} \times \sqrt{3}$ unit cell. (b) The surface Brillouin zone of the $\sqrt{3} \times \sqrt{3}$ unit cell.

per unit cell: one atom occupies a hollow H₃ site and the other three are in off-centered T_1 sites thereby forming a trimer just above the top Si layer, as shown in Fig. 1(a). As a consequence, the Pb adlayer appears to be compressed by 5% compared with the bulk Pb(111) plane.

The bottom bilayer of Si atoms and the hydrogen layer are kept fixed to simulate the bulk environment. All other atoms are allowed to relax freely (both in-plane and along the stacking direction) until the forces are less than 0.025 eV/Å. The force criterion is sufficient to ensure the bond lengths and the interlayer distances in the substrate. The H-Si distance is determined in a calculation for a Si film saturated by H on both sides. The bond lengths, $d_{\text{Pb(H)−Pb}}$, $d_{\text{Pb−Pb}}$, and $d_{\text{Pb−Si}_1}$, calculated both with and without SOC are given in Table I together with available data from other first-principles calculations [27,28]. The bond length between a Pb atom in the hollow site and other Pb atoms, $d_{\text{Pb(H)−Pb}}$, is close to the Pb-Pb covalent bond length, 2.94 Å [37]. The distance between Pb atoms in the trimers is greater than $d_{\text{Pb(H)−Pb}}$ and closer to the metallic Pb bond length, 3.50 Å. The Pb-Si length is found to be in the experimental covalent bond interval obtained for lead adatoms located in the top sites of the Si(111)-($\sqrt{7} \times \sqrt{3}$)-Pb structure, $d_{\text{Pb−Si}}^{\text{exp}} = 2.65$–2.93 Å [37]. The Pb overlayer, on the whole, forms a slightly corrugated surface above (~2.6 Å) the Si substrate. Each adatom in the trimers forms a covalent

TABLE I. Bond lengths (in Å): $d_{Pb(H)-Pb}$, d_{Pb-Pb}, and d_{Pb-Si_1} as well as Δz, the height difference between atoms in the interface. The values taken from Ref. [27] were obtained for a 12-layer substrate film (12Si) using the projector augmented-wave method and the generalized gradient approximation (GGA) for the exchange-correlation functional. In the present calculation and in Ref. [28] a six-layer substrate film (6Si) was used and the local density approximation in the pseudopotential approach.

	w/o SOC	w/o SOC[b]	SOC	SOC[a]
$d_{Pb(H)-Pb}$	3.05	3.03	3.02	3.101
d_{Pb-Pb}	3.34	3.38	3.35	
d_{Pb-Si_1}	2.79		2.79	2.882
$\Delta z_{Pb(H)-Si_1}$	2.59	2.60	2.63	2.649
$\Delta z_{Si_1-Si_2}$	0.80	0.82	0.80	

[a]GGA, the projector augmented-wave method Ref. [27].
[b]LDA, pseudopotential plane-wave method Ref. [28].

bond with an underlying substrate atom while the Pb atoms in hollow sites are only bonded metallically to other Pb atoms. We note that the structural parameters are hardly influenced by the spin-orbit coupling (see Table I).

III. RESULTS AND DISCUSSION

A. Electron-phonon coupling

We have evaluated the momentum-averaged strength of the e-ph interaction, $\lambda(E)$, at various energies below and above E_F. Figure 2 shows the band structure calculated both with [Fig. 2(a)] and without [Fig. 2(b)] SOC to point out the crucial influence of spin-orbit interaction on the dispersion of Pb electronic bands. The SBZ symmetry points are given in Fig. 1(b). The Pb electronic bands are of p character within the substrate band gap. Near E_F they are completely of $p_{x,y}$ symmetry, which indicates the in-plane metallic Pb-Pb bonding. A detailed description of the band dispersion for the (4/3)-monolayer structure of Pb on Si(111) can be found in Ref. [27].

The influence of spin-orbit coupling on the strength of the e-ph interaction and the density of electronic states, $N(E)$, is shown in Figs. 2(c) and 2(d). The variation of $\lambda(E)$ and $N(E)$ with energy suggests that the strength of the e-ph coupling is generally proportional to the number of electronic states available for scattering processes (phase space). It also follows from the ratio $\lambda(E)/N(E)$ shown in Fig. 2(e). Below E_F, the e-ph coupling grows only gradually, while $N(E)$ increases sharply with binding energy due to the contribution of substrate electronic bands. The reason of these different behaviors is that Si bands contribute little to the phonon-mediated scattering compared to the Pb adlayer bands.
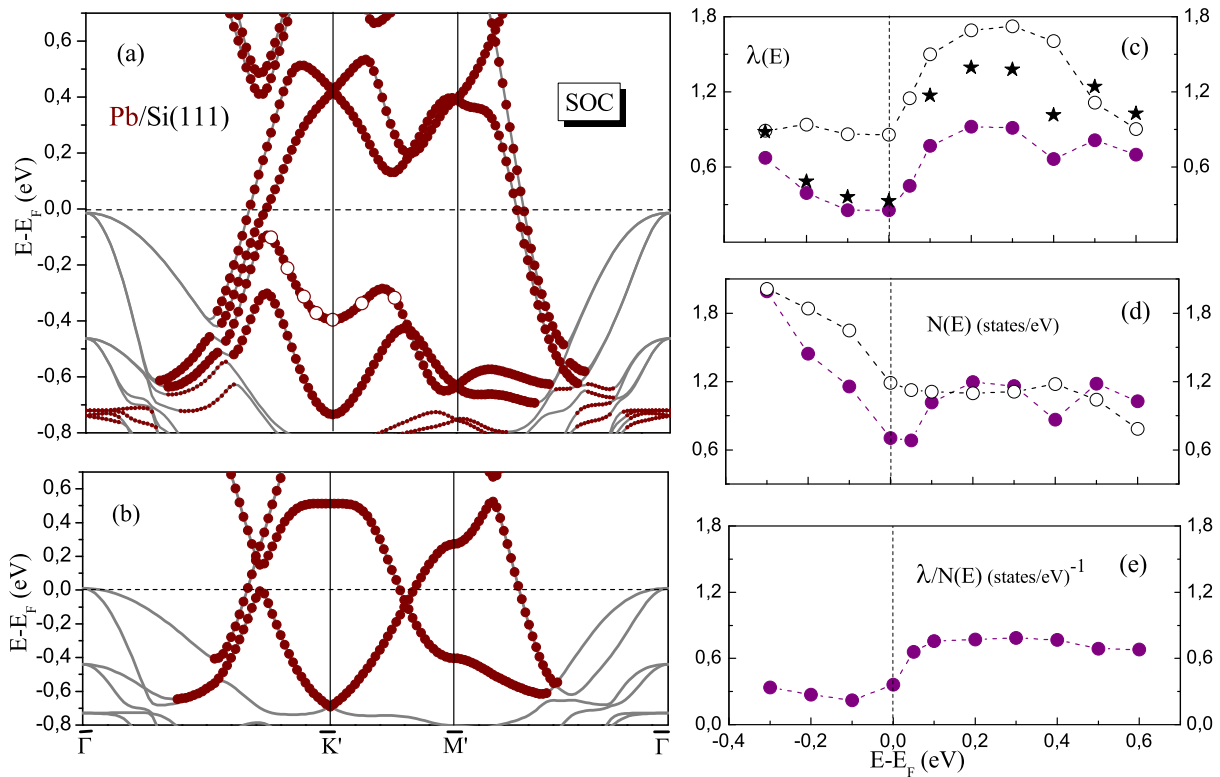

FIG. 2. (a), (b) Band structure of the H_3 phase formed by (4/3)-ML of Pb on Si(111) obtained with (a) and without (b) SOC. Brown circles show electronic bands formed mainly by Pb orbitals. (a) The occupied Pb electronic states, for which the strength of the e-ph interaction λ_{ki} is calculated, are marked by open circles. (c) Electron–phonon coupling parameter $\lambda(E)$ averaged over electron momentum. (d) Electronic density of states $N(E)$, and (e) $\lambda(E)/N(E)$ as a function of energy. The full and open circles correspond to the calculations with and without SOC, respectively. Stars (c) give the values of $\lambda(E)$ evaluated using electronic states and e-ph matrix elements from the calculation including SOC and combining them with the phonon spectrum from the scalar relativistic calculation.

The value of $\lambda(E_F) = 0.86$ obtained without SOC agrees reasonably with the findings of other *ab initio* scalar relativistic calculations: $\lambda(E_F) = 0.72$ [20] and $\lambda(E_F) = 0.737$ [21]. Using such large values of $\lambda(E_F)$ in the Allen-Dynes equation, for example, to estimate the superconduction transition temperature [20] results in a very good agreement with the experimental value of 1.83 K [3].

However, our calculations show that the influence of relativistic corrections on the strength of e-ph coupling is profound and $\lambda(E)$ is strongly overestimated in the scalar relativistic calculations unlike bulk lead [25] and freestanding Pb films [22], where the inclusion of SOC results in a large enhancement ($\sim$44% at the Fermi level of bulk Pb) of the coupling strength. In the dense Si(111)-supported Pb($\sqrt{3} \times \sqrt{3}$) phase calculation the relativistic corrections decrease $\lambda(E)$ by 25–70 % depending on electron energy. Thus the value of $\lambda(E_F)$ is reduced by up to a factor of three down to 0.26.

Since there are many factors that interfere, the influence of SOC on the e-ph interaction is rather intricate [25]. In the following we will address the effect of spin-orbit coupling on two major factors, which determine $\lambda(E)$: the density of electronic states and the e-ph spectral function (the e-ph matrix elements).

1. Density of electronic states

On the one hand, the SOC-induced changes in the dispersion of Pb electronic bands (see Figs. 2(a) and 2(b) and Ref. [27]) are enough to have an appreciable influence on phonon-mediated electronic transitions thereby affecting deeply e-ph matrix elements. The spin degeneracy of Pb electronic bands, in particular, is lifted over the SBZ except the high-symmetry points. At the $\overline{K'}$ point the spin-orbit splitting in the highest occupied Pb electronic band comes up to 340 meV (300 meV [27]). The band structure in addition exhibits a large pseudogap of 415 meV (385 meV [27]) along the $\overline{K'M'}$ line. Both the spin-orbit splitting and the pseudogap opening are caused by the SOC-induced strong hybridization of Pb $p_{x,y}$ and p_z orbitals and the resulting asymmetry of surface charge distribution [27,38].

On the other hand, the density of electronic states changes. The largest differences due to the spin-orbit coupling are found just below and at E_F. For example, $N(E_F)$ decreases by $\sim$40% unlike in bulk Pb and in freestanding Pb films where an increase of 2–6 % due to the SOC was found [22,25].

In fact, in the case of freestanding Pb films [22] or (1×1) Pb/Si(111) films of 10–22 ML thickness [39] the first-principles calculations showed a minor influence of spin-orbit coupling on the band dispersion. The DFT calculation of surface formation energies and the density of electronic states for different structures of 1/3 ML of Pb on Si(111) showed that their valence electronic structure is hardly affected by SOC too [44]. However, this is not the case for the dense H_3 phase considered here. Although the SOC-induced modifications of $N(E)$ are small at some energies, they are large in particular for E close to E_F, and the effect of SOC on the dispersion of Pb electronic bands is so significant that it can not be ignored. These findings are in accord with a thorough study of how the (4/3)-ML Pb/Si(111) electronic structure is affected by SOC [27].

2. Lattice dynamics and Eliashberg spectral function

Another factor that affects the variation of $\lambda(E)$ is lattice vibrations. The phonon dispersion curves calculated with the inclusion of SOC are shown in Fig. 3(a). To obtain a more reliable description of modes the substrate thickness was increased up to 60 layers by adding bulklike layers with force constants taken from an *ab initio* calculation of bulk Si using a $(12 \times 12 \times 12)$ **q**-point mesh. The phonon modes localized mainly on Pb atoms lie below 12 meV, while the vibrations of substrate atoms occupy the high-frequency region extending up to 72 meV. The modes with predominantly shear-vertical displacements of lead atoms (along the normal to the surface) are shown with full circles in the figure. A detailed description of the phonon dispersion obtained without taking into account SOC can be found in Ref. [40]. The dynamics of vibrations localized in a (4/3)-monolayer of Pb on Si(111) was studied using density-functional theory and molecular dynamics methods employing the generalized gradient approximation for the exchange-correlation functional.

In bulk Pb [41,42] and freestanding Pb(111) films [22] the inclusion of spin-orbit interaction produces a large shift of the phonon spectra toward lower frequencies, which promotes a considerable increase of $\lambda(E)$. In the bulk, the average softening is about 8–15 % depending on mode polarization [25]. In the freestanding Pb(111) films, the SOC-induced difference in phonon energies amounts to 24% in the vicinity of the SBZ boundary regardless of the film thickness [22]. The lattice dynamics of the dense Si(111)-Pb($\sqrt{3} \times \sqrt{3}$) phase is found (i) to be less affected by SOC and (ii) the effect is opposite to that observed in freestanding Pb(111) films.

The inclusion of SOC results mainly in a stiffening of the low-energy modes, which can be clearly seen in the density of phonon states, Fig. 3(b). This frequency region is very important in the e-ph coupling due to the definition of λ, Eq. (1). The SOC-induced stiffening is also visual in the e-ph spectral functions $\alpha^2 F(\omega)$. Figures 3(d) and 3(f) show the spectral functions calculated at E_F and $(E - E_F) = +0.1$ eV both with (full circles) and without (open circles) SOC. First, the position of peaks in the low-energy region is shifted and, in addition, the weight of many peaks is reduced especially at the Fermi level. Both processes promote a decrease of $\lambda(E)$.

Also shown are the spectral functions obtained with the phonon spectrum taken from the scalar relativistic calculation (hatched areas) to estimate the importance of the phonon frequency shift. The corresponding values of $\lambda(E)$ are given by stars in Fig. 2(c). At E_F and just below the Fermi level, where the contribution of low-energy phonons to the e-ph scattering is not large (with the inclusion of SOC), the frequency shift results mainly in a shift of a peak $\sim$3.5 meV, which is determined by vibrations of Pb atoms along the normal to the surface, toward lower frequencies. The values of $\lambda(E)$ show a slight increase compared to the results obtained with SOC, see Fig. 2(c). At energies inside the substrate energy gap (above E_F), the low-energy peaks of $\alpha^2 F(\omega)$ are not only shifted but also enhanced, Fig. 3 (f), and the strength of e-ph interaction gets enhanced by 50%.

It is obvious that for a single layer of Pb on Si(111) the effect of substrate should be important [43]. A strong covalent bond between Pb and Si atoms at the interface [3,44]
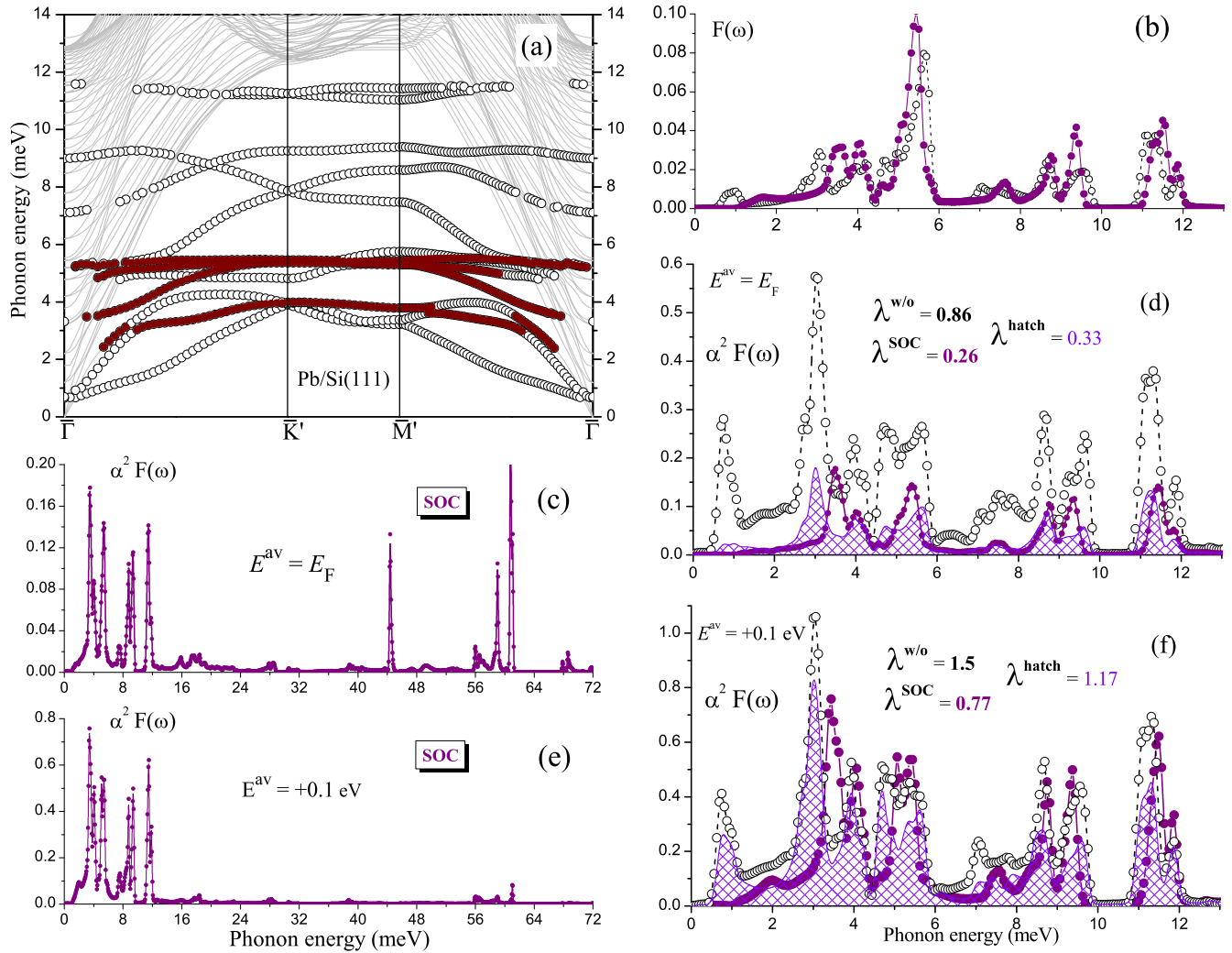
FIG. 3. (a) Phonon dispersion curves for a 60-layer Si(111) film with (4/3)-ML of Pb arranged in the $\sqrt{3} \times \sqrt{3}$ structure on the top of the surface. The data were obtained with inclusion of SOC. The phonon spectrum is given up to 14 meV to show mainly Pb localized modes (circles). The full circles indicate Pb phonons with shear-vertical polarization (along the surface normal). (b) Phonon density of states $F(\omega)$ calculated both with (full circles) and without (open circles) spin-orbit interaction. (c)–(f) Eliashberg spectral functions, $\alpha^2 F(\omega)$, calculated at the Fermi energy (c), (d) and at $(E - E_F) = +0.1$ eV (e), (f) with (full circles) and without (open circles) spin-orbit coupling. Also shown is $\alpha^2 F(\omega)$ evaluated using all the data calculated with SOC except for the phonon spectrum taken from the scalar relativistic calculation (hatched areas) (d), (f). The corresponding λ are shown by stars in Fig. 2(c).

favors a stiffening of phonon modes and as a consequence, a decreasing of the e-ph coupling strength. However, a direct substrate contribution to the e-ph coupling is found to be small. Figures 3(c) and 3(e) show spectral functions calculated at the Fermi energy and at $(E - E_F) = +0.1$ eV, respectively, for the whole phonon spectrum including the Si substrate modes. It is evident that a decisive contribution to the e-ph interaction comes from the Pb-localized phonons while the contribution from high-frequency substrate modes is minor because λ scales approximately as $1/\omega^2$, Eq. (1).

3. Estimation of T_c

The scanning tunneling microscopy measurements [3] demonstrated the existence of a superconducting phase for the (4/3)-ML of Pb on Si(111) with $T_c = 1.83$ K. We note that such measurements probe electronic states at the Fermi level.

Among the factors that determine T_c is the strength of the e-ph interaction. The calculated value of $\lambda(E_F) = 0.26$ is too small to give such T_c. The question arises as to whether the positions of E_F in the experiment and in the calculation coincide with respect to the substrate valence band edge.

In the experiment, E_F lies well within the Si band gap and therefore the Fermi surface is exclusively formed by Pb electronic bands. Unfortunately, the precise position of E_F is not given in Ref. [3], but as follows from the energy bands measured by high-resolution angle-resolved photoemission spectroscopy (Fig. 4, Ref. [3]) E_F is ∼0.1 eV above the valence band maximum (VBM) at the $\overline{\Gamma}$ point. The position of the Fermi level in the respective phase was also estimated using ultraviolet photoemission spectroscopy [45,46]. It was found that E_F is at 0.09 ± 0.03 eV above the substrate valence band edge.

In *ab initio* calculations, both in the present one and in another first-principles investigation [27], the Fermi level lies
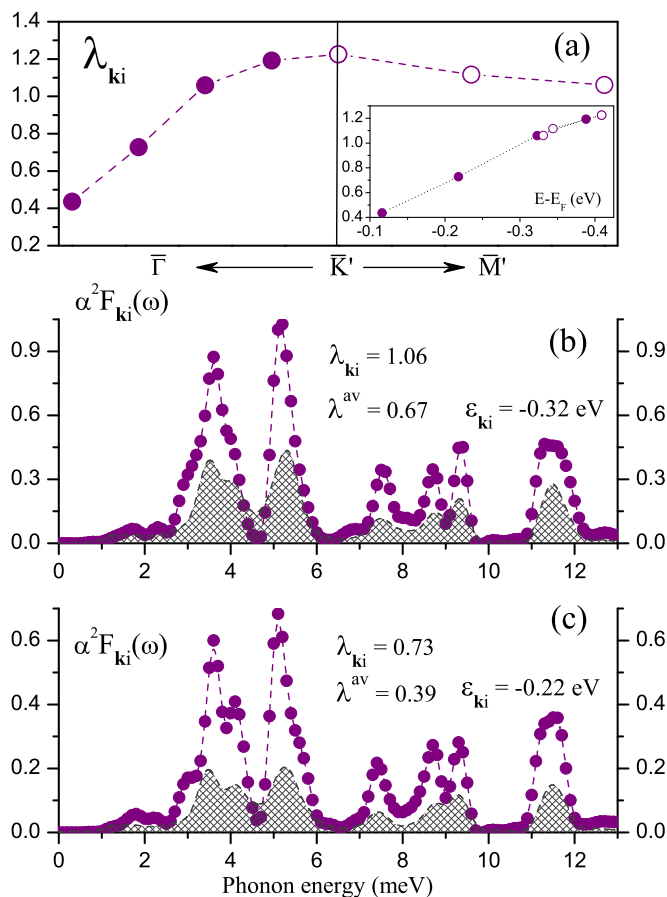
FIG. 4. (a) Electron-phonon coupling parameter $\lambda_{\mathbf{k}i}$ as a function of momentum for the occupied Pb electronic states marked by open circles in Fig. 2(a) in the $\overline{\Gamma K'}$ and $\overline{K'M'}$ symmetry directions. The data were obtained with SOC included. The energy dependence of $\lambda_{\mathbf{k}i}$ is shown in the insert. (b), (c) Eliashberg spectral functions, $\alpha^2 F_{\mathbf{k}i}(\omega)$ (circles), calculated for electronic states at $\epsilon_{\mathbf{k}i} = -0.32$ eV (b) and $\epsilon_{\mathbf{k}i} = -0.22$ eV (c). Hatched areas show the corresponding spectral functions at the same binding energies but averaged over electron momentum.

very close to the substrate valence band maximum. Of course, the LDA (and also GGA) may underestimate the Si band gap, but the reduction in the size of the gap is not important for analyzing the e-ph interaction in the system of interest. The main point is the position of E_F relative to the substrate valence band edge. As follows from Fig. 2(d), the density of electronic states decreases sharply at the Fermi energy. The drop in $N(E)$ is observed only when SOC is taking into account. The density of Si electronic states is not affected by SOC, therefore this sudden drop is due to a decrease in the density of Pb electronic states. The decrease is so strong that although Si bands start to contribute, the total $N(E)$ decreases. As a consequence the value of $\lambda(E_F)$ is much smaller than $\lambda(E)$ inside the Si band gap, as seen in Fig. 2(c).

We have estimated the critical temperature at the experimental position of Fermi level, at ~ 0.1 eV above the substrate valence band edge. T_c was obtained by solving the linearized gap equation of the Eliashberg theory [47,48]. To get an accurate value two input parameters are needed, $\alpha^2 F(\omega)$ and

μ^*, an effective Coulomb repulsion. The spectral function is known from the calculation, but it is not clear which value of μ^* should be used. In bulk Pb, the effective Coulomb interaction parameter [49,50] is assumed to be in the range of 0.1–0.12. Although in the 2D limit the electronic screening is usually reduced compared to the bulk, in the case of lead, it is shown that even a one-layer free-standing Pb(111) film should exhibit the screening typical for bulk lead [51].

We used typical bulk values of μ^* (0.1–0.12) and the reference frequency $\omega_c \approx 5$ meV, which is close to the logarithmic averaged phonon frequency [52]. The calculated T_c varies between 1.67 K and 2.03 K with μ^*. When taking $\mu^* = 0.11$, $T_c = 1.84$ K is very close to the measured value of 1.83 K. Thus it is likely that the cause of the discrepancy in the critical temperature between theory and experiment is the position of the Fermi level.

B. Band-resolved electron-phonon coupling

An attempt to estimate the electron-phonon coupling parameter from experiment was reported by Zhang *et al.* [3]. The temperature-dependent photoemission spectrum at different temperatures (78–200 K) was measured for an occupied Pb electronic state at energy $(E - E_F) \sim -300(350)$ meV using variable-temperature high-resolution angle-resolved photoemission spectroscopy [3]. To avoid the influence of Si valence bands, the photoemission spectra was taken at $\mathbf{k}_{xy} = 0.38$ Å^{-1} (in the $\overline{\Gamma K'M}$ symmetry direction). The strength of e-ph interaction was obtained by fitting the temperature-dependent linewidth.

The strength of the e-ph interaction for a particular electron state with momentum $\mathbf{k}$ and band index i, $\lambda_{\mathbf{k}i}$, is defined using the corresponding state-dependent Eliashberg spectral function $\alpha^2 F_{\mathbf{k}i}(\omega)$ in Eq. (1)

$$\alpha^2 F_{\mathbf{k}i}(\omega) = \sum_{\mathbf{q},\nu,f} \delta(\epsilon_{\mathbf{k}+\mathbf{q}f} - \epsilon_{\mathbf{k}i}) \left| g_{\mathbf{k}+\mathbf{q}f,\mathbf{k}i}^{\mathbf{q}\nu} \right|^2 \delta(\omega - \omega_{\mathbf{q}\nu}). \quad (3)$$

Here the quasielastic approximation is used: $\delta(\epsilon_{\mathbf{k}+\mathbf{q}f} - \epsilon_{\mathbf{k}i} \mp \omega_{\mathbf{q},\nu}) \approx \delta(\epsilon_{\mathbf{k}+\mathbf{q}f} - \epsilon_{\mathbf{k}i})$. The sum is carried out over final electron states and all possible phonon modes $(\mathbf{q},\nu)$. We have calculated $\lambda_{\mathbf{k}i}$ for a number of electronic states in the occupied Pb surface band marked by open circles in Fig. 2(a).

First, we find that $\lambda_{\mathbf{k}i}$ varies depending on binding energy rather than electronic momentum and exhibits a monotonic increase with binding energy [Fig. 4(a), insert], following essentially the almost linear increase in the density of states, Fig. 2(d). This suggests that the coupling strength of an electronic state is mainly determined by the number of available final electronic states.

Second, the calculated $\lambda_{\mathbf{k}i}$ are markedly stronger than the corresponding value averaged over electron momentum [see Figs. 4(b) and 4(c)]. The point is that the phonon-mediated scattering inside substrate electronic bands is less effective giving a negligible contribution to $\lambda_{\mathbf{k}i}$ as compared to the e-ph matrix elements for Pb electronic states.

At binding energies about 200–350 eV the calculated strength of the e-ph interaction, 0.7–1.1, is very close to the value extracted from the measurements, $\lambda^{\exp} = 1.07 \pm 0.13$, but quite distinct from the average value at E_F. This suggests that the state chosen in the experiment is not a good

representative for the average coupling strength at E_F relevant for superconductivity.

IV. SUMMARY

We have studied the effect of spin-orbit interaction on the electron-phonon coupling in a (4/3)-monolayer of Pb on Si(111) using first-principles calculations in the density-functional perturbation formalism.

The calculations show that the influence of SOC on the strength of e-ph interaction is profound and the e-ph coupling parameter is strongly overestimated in the scalar relativistic calculations. At the Fermi level, the value of $\lambda(E_F)$ is lowered by more than a factor of three with the inclusion of SOC unlike the case of bulk lead or freestanding Pb films, where a large enhancement of the e-ph coupling parameter is observed. The effect of spin-orbit interaction on phonon-mediated electronic transitions is largely determined by the SOC-induced modification of Pb electronic band structure at but not restricted to E_F, which is so significant that it can not be ignored. Another factor is a stiffening of lower-energy phonon modes. Both processes account for a weakening of the e-ph

coupling strength. However, at the position of experimental E_F ($\sim$+0.1 eV) a good agreement with the experiment data is obtained just because the SOC-induced decreasing of $\lambda(E)$. Therefore, it is mandatory to take the spin-orbit interaction into account in determining the superconducting transition temperature.

The strength of electron-phonon interaction in occupied Pb bands exhibits a monotonic increase with binding energy and is mainly determined by the available phase space. The state-dependent coupling is found to be stronger than the value of $\lambda(E)$ averaged over electron momentum at the same energy and agrees well with available experimental data.

[1] S. Y. Qin, J. Kim, Q. Niu, and C. K. Shih, Science **324**, 1314 (2009).

[2] Ph. Hofmann, I. Yu. Sklyadneva, E. D. L. Rienks, and E. V. Chulkov, New J. Phys. **11**, 125005 (2009).

[3] T. Zhang, P. Cheng, W. J. Li, Yu.-J. Sun, G. Wang, X. G. Zhu, K. He, L. Wang, X. Ma, X. Chen, Y. Wang, Y. Liu, H. Q. Lin, L. F. Jia, and Q. K. Xue, Nature Phys. **6**, 104 (2010).

[4] T. Hirahara, T. Nagao, I. Matsuda, G. Bihlmayer, E. V. Chulkov, Yu. M. Koroteev, and S. Hasegawa, Phys. Rev. B **75**, 035422 (2007).

[5] G. L. Lay, J. Peretti, M. Hanbucken, and W. S. Yang, Surf. Sci. **204**, 57 (1988).

[6] Y. Guo, Y. F. Zhang, X. Y. Bao, T. Z. Han, Z. Tang, L. X. Zhang, W. G. Zhu, E. Wang, Q. Niu, Z. Qiu, J. F. Jia, Z. X. Zhao, and Q.-K. Xue, Science **306**, 1915 (2004).

[7] D. Eom, S. Qin, M. Y. Chou, and C. K. Shih, Phys. Rev. Lett. **96**, 027005 (2006).

[8] M. M. Özer, J. R. Thompson, and H. H. Weitering, Nature Phys. **2**, 173 (2006).

[9] C. Brun, I.-P. Hong, F. Patthey, I. Y. Sklyadneva, R. Heid, P. M. Echenique, K. P. Bohnen, E. V. Chulkov, and W.-D. Schneider, Phys. Rev. Lett. **102**, 207002 (2009).

[10] A. Mans, J. H. Dil, A. R. H. F. Ettema, and H. H. Weitering, Phys. Rev. B **72**, 155442 (2005).

[11] Y. F. Zhang, J. F. Jia, T. Z. Han, Z. Tang, Q. T. Shen, Y. Guo, Z. Q. Qiu, and Q. K. Xue, Phys. Rev. Lett. **95**, 096802 (2005).

[12] P. S. Kirchmann and U. Bovensiepen, Phys. Rev. B **78**, 035437 (2008).

[13] N. Miyata, K. Horikoshi, T. Hirahara, S. Hasegawa, C. M. Wei, and I. Matsuda, Phys. Rev. B **78**, 245405 (2008).

[14] I. Yu. Sklyadneva, G. Benedek, E. V. Chulkov, P. M. Echenique, R. Heid, K.-P. Bohnen, and J. P. Toennies, Phys. Rev. Lett. **107**, 095502 (2011).

[15] R. Díez Muiño, S. Sánchez-Portal, V. M. Silkin, E. V. Chulkov, and P. M. Echenique, Proc. Natl. Acad. Sci. U. S. A. **108**, 971 (2011).

[16] A. A. Shanenko, M. D. Croitoru, and F. M. Peeters, Phys. Rev. B **75**, 014519 (2007).

[17] Y. Chen, A. A. Shanenko, and F. M. Peeters, Phys. Rev. B **85**, 224517 (2012).

[18] F. Yndurain and M. P. Jigato, Phys. Rev. Lett. **100**, 205501 (2008).

[19] J. Noffsinger and M. L. Cohen, Phys. Rev. B **81**, 214519 (2010).

[20] J. Noffsinger and M. L. Cohen, Solid State Commun. **151**, 421 (2011).

[21] G. Q. Huang, New J. Phys. **13**, 093023 (2011).

[22] I. Yu. Sklyadneva, R. Heid, K.-P. Bohnen, P. M. Echenique, and E. V. Chulkov, Phys. Rev. B **87**, 085440 (2013).

[23] I.-P. Hong, C. Brun, F. Patthey, I. Y. Sklyadneva, X. Zubizarreta, R. Heid, V. M. Silkin, P. M. Echenique, K. P. Bohnen, E. V. Chulkov, and W.-D. Schneider, Phys. Rev. B **80**, 081409(R) (2009).

[24] M. Ligges, M. Sandhofer, I. Yu. Sklyadneva, R. Heid, K.-P. Bohnen, S. Freutel, L. Rettig, P. Zhou, P. M. Echenique, E. V. Chulkov, and U. Bovensiepen, J. Phys.: Condens. Matter **26**, 352001 (2014).

[25] R. Heid, K.-P. Bohnen, I. Yu. Sklyadneva, and E. V. Chulkov, Phys. Rev. B **81**, 174527 (2010).

[26] I. Y. Sklyadneva, R. Heid, P. M. Echenique, K.-B. Bohnen, and E. V. Chulkov, Phys. Rev. B **85**, 155115 (2012).

[27] X. Y. Ren, H. J. Kim, S. Yi, Y. Jia, and J. H. Cho, Phys. Rev. B **94**, 075436 (2016).

[28] T. L. Chan, C. Z. Wang, M. Hupalo, M. C. Tringides, Z. Y. Lu, and K. M. Ho, Phys. Rev. B **68**, 045410 (2003).

[29] P. B. Allen and M. L. Cohen, Phys. Rev. **187**, 525 (1969).

[30] L. Hedin and B. I. Lundqwist, J. Phys. C: Solid State Phys. **4**, 2064 (1971).

[31] D. Vanderbilt, Phys. Rev. B **32**, 8412 (1985).

[32] S. G. Louie, K. M. Ho, and M. L. Cohen, Phys. Rev. B **19**, 1774 (1979).

[33] R. Heid and K.-P. Bohnen, Phys. Rev. B **60**, R3709 (1999).

[34] N. E. Zein, Sov. Phys. Solid State **26**, 1825 (1984) [Fiz. Tverd. Tela (Leningrad) **26**, 3028 (1984)].

[35] S. Baroni, S. de Gironcoli, A. D. Corso, and P. Giannozzi, Rev. Mod. Phys. **73**, 515 (2001).

[36] A. G. Beattie and J. E. Schirber, Phys. Rev. B **1**, 1548 (1970).

[37] C. Kumpf, O. Bunk, J. H. Zeysing, M. M. Nielsen, M. Nielsen, R. L. Johnson, and R. Feidenhans, Surf. Sci. **448**, L213 (2000).

[38] S. W. Kim, C. Liu, H. J. Kim, J. H. Lee, Y. Yao, K. M. Ho, and J. H. Cho, Phys. Rev. Lett. **115**, 096401 (2015).

[39] T. Stein, H. Eisenberg, L. Kronik, and R. Baer, Phys. Rev. Lett. **105**, 266802 (2010).

[40] S. Sakong, P. Kratzer, S. Wall, A. Kalus, and M. Horn-vonHoegen, Phys. Rev. B **88**, 115419 (2013).

[41] A. D. Corso, J. Phys.: Condens. Matter **20**, 445202 (2008).

[42] M. J. Verstraete, M. Torrent, F. Jollet, G. Zérah, and X. Gonze, Phys. Rev. B **78**, 045119 (2008).

[43] D. A. Luh, T. Miller, J. J. Paggel, and T. C. Chiang, Phys. Rev. Lett. **88**, 256802 (2002).

[44] M. Rafiee and S. J. Asadabadi, Comput. Mater. Sci. **47**, 584 (2009).

[45] X. Tong, K. Horikoshi, and S. Hasegawa, Phys. Rev. B **60**, 5653 (1999).

[46] H. H. Weitering, A. R. H. F. Ettema, and T. Hibma, Phys. Rev. B **45**, 9126 (1992).

[47] G. Grimvall, *The Electron-Phonon Interaction in Metals* (North-Holland, Amsterdam, 1981).

[48] G. Bergmann and D. Rainer, Z. Phys. **263**, 59 (1973).

[49] W. L. McMillan, Phys. Rev. **167**, 331 (1968).

[50] G. P. Carbotte, Rev. Mod. Phys. **62**, 1027 (1990).

[51] P. S. Kirchmann, L. Rettig, X. Zubizarreta, V. M. Silkin, E. V. Chulkov, and U. Bovensiepen, Nature Phys. **6**, 782 (2010).

[52] P. B. Allen and R. C. Dynes, Phys. Rev. B **12**, 905 (1975).